

Large Size Microneedle Patch to Deliver Lidocaine through Skin

Himanshu Kathuria¹ · Hairui Li¹ · Jing Pan¹ · Seng Han Lim¹ · Jaspreet Singh Kochhar¹ · Chunyong Wu² · Lifeng Kang¹ 

Received: 25 April 2016 / Accepted: 30 June 2016
© Springer Science+Business Media New York 2016

ABSTRACT

Purpose Current topical treatments using lidocaine (LD) for analgesia have limited applications due to their delayed analgesic actions, resulted from slow drug permeation through skin. The aim of this study is to fabricate a large size microneedle (MN) array patch containing LD, with fast onset of action, for the treatment of acute and chronic pain.

Methods The MN patch was developed through photolithography and tested for its mechanical characteristics. *In vitro* and *in vivo* skin permeation, plasma pharmacokinetics, histology and skin irritation testing have also been performed for the MN patches.

Results The MN have a mechanical strength of 10–30 N and more than 90% of the microneedles on the patch penetrated skin. It was shown that LD permeated through skin within 5 min of patch application. Subsequently, the *in vivo* skin permeation study using a porcine model showed that LD administered by the MN patch was able to achieve the therapeutic level locally within 10 min and sustained for 8 h. It shows most of the drug diffuses perpendicularly against skin, with little lateral diffusion. After skin permeation LD remains within skin and unquantifiable amount of LD was found in the plasma of the pigs. Minor skin irritations were observed after 6 h

of microneedle contact. However, the skin irritations resolved within 1 day following the removal of MN patch.

Conclusion The large size MN patches showed fast onset and sustained delivery of LD through skin, potentially useful to increase the application scope of topical LD for pain management.

KEY WORDS drug diffusion · lidocaine · microneedle · pain · skin permeation · transdermal patch

ABBREVIATIONS

BL	Backing layer
DSC	Differential scanning calorimetry
H & E	Hematoxylin and eosin
HaCaT	Human adult low calcium high temperature
HDF	Human dermal fibroblasts
HEK293	Human embryonic kidney 293
HMP	2-hydroxy-2-methyl-propiofenone
LD	Lidocaine
MN	Microneedle
PBS	Phosphate-buffered saline
PEGDA	Poly(ethylene glycol) diacrylate
TMSPMA	3-(Trimethoxysilyl) propyl methacrylate
UV	Ultraviolet

Electronic supplementary material The online version of this article (doi:10.1007/s11095-016-1991-4) contains supplementary material, which is available to authorized users.

✉ Lifeng Kang
lkang@nus.edu.sg

¹ Department of Pharmacy, National University of Singapore, Singapore 117543, Singapore

² Department of Pharmaceutical Analysis, China Pharmaceutical University, Nanjing 210009, China

INTRODUCTION

The occurrence of pain is very common during invasive clinical procedures, such as injections, surgeries, venipuncture or catheterization. To address this clinical situation, local anesthetics are applied on the site locally to provide analgesia before initiating the procedures. Lidocaine (LD) is a widely used local anesthetic, routinely used for the management of pre and postoperative procedural pain conditions either alone or in combination with other drugs. The anti-nociceptive

actions of LD has been known to arise from multifaceted mechanisms, because of which it is safe to administer LD via different routes for a variety of medical conditions (1). Although intravenous administration of LD is highly efficacious for pre-operative and post-operative pain management (2, 3), it causes systemic side effects, inconvenience and may lead to non-compliance in patients, especially the pediatric and geriatric populations. Oral dosing of LD may pose a problem for geriatric population who have been often already loaded with a high pill burden or may have difficulties in swallowing, similar to the pediatric population. To this end, transdermal route for LD administration has been a new focus of research for pre-operative and post-operative pain management.

Creams, gels and transdermal patches, etc. are widely utilized for pain management. However, the application time required by them to produce sufficient analgesia may be unacceptable to many, including doctors, patients and nurses. For instance, EMLA cream containing 5% LD is typically used on the skin prior to venipuncture. It takes approximately 120 min to produce analgesia (4); whereas EMLA transdermal patch takes about 60 min to produce analgesia. The lack of rapid action for such formulations is primarily due to a protective epithelial barrier of the skin. In a recent meta-analysis of prospective controlled trials, it was shown that the application of transdermal LD patch is not an effective adjunct for acute and postoperative pain management (5). This calls for new transdermal or topical approach for LD drug delivery which is rapid in its onset of action.

Physical methods such as iontophoresis (6), sonophoresis (7, 8), laser pretreatment (9) and magnetophoresis (10) have been shown to achieve desired analgesic effect in less time than conventional dosage forms. However, the lack of established safety data for such devices is a concern (11–13). Ernst *et al.* reported a significant difference in the formation of more granuloma and granulation tissue in the iontophoresis group as compared to the injected LD control group (14). For chemical methods, Nanorap, a new nanotechnological formulation of LD with prilocaine for use in topical anesthesia has been shown to provide analgesia after 10 min of application with >30% pain reduction (15). Various chemical penetration enhancers have also been studied for the enhancement of LD skin permeation (16–19). Recently Stahl *et al.* showed that with MN pretreatment, there is increased LD skin permeation compared to the use of chemical enhancers (19).

If only MN pre-treatment is considered, a single pretreatment just before application of the topical formulation does not work for long as it subsequently lead to premature closure of MN-created pores and slow down the permeation thereafter. Hence, often, MN pretreatment can only maintain the desired analgesic effect for a short period of time. Zhang, Y. *et al.* has shown that using MN coated with a drug, one can achieve rapid therapeutic level (20). However, it

cannot maintain the therapeutic level because of low drug loading.

MN patch previously developed from our group showed potential to a fast and sustained skin permeation of LD (21). Fast and sustained skin permeation were the outcomes of persistent MN penetration into the skin and high drug loading in the MN arrays. However, previously, the patch size was small to produce analgesia on big area of skin. Moreover, it was lacking the pre-clinical *in vivo* skin permeation data for the microneedle integrated transdermal patch. Currently there is no such method of fabrication to produce the large size MN patch. For clinical applications, it is easier to apply the single patch than multiple patches at required site. The large size patch can be easily utilized for upper and lower back, thighs, hands, chest, etc. which actually requires larger area of administration in various clinical pain management, as seen from commercially available LD transdermal patches (>100 cm²), for e.g., Lidoderm (patch size 10 cm × 14 cm <140 cm²>).

In this study, we developed large size polymeric MN patch using photolithography. The MN patches were characterized for their physical and mechanical characteristics. The *in vitro* skin permeation was performed for MN patches to observe the effect of microneedle on skin permeation. To further assess its efficacy and safety, *in vivo* skin permeation was also conducted by using a porcine model.

EXPERIMENTAL SECTION

Materials and Animals

Poly(ethylene glycol) diacrylate, PEGDA (M_n = 258), 2-hydroxy-2-methyl-propiofenone (HMP), Proteinase K, Ammonium Hydroxide, formic acid 50%, 3-(Trimethoxysilyl) propyl methacrylate; TMSPMA were purchased from Sigma-Aldrich (St. Louis, MO, USA). HPLC-grade Isopropyl alcohol, acetonitrile and methanol were supplied by Tedia, USA. Lidocaine was purchased from TCI, Japan. Polyethylene glycol 200 (PEG 200) was purchased from Alfa Aesar (Ward Hill, MA, USA). Water used in these studies was purified using Millipore Direct-Q. Phosphate-buffered saline (PBS) ultra-pure grade was obtained from Vivantis, Malaysia.

Young adult female swine (Yorkshire X, Holland), ranging from 25 to 40 kg were used for the study. The animals were housed in an air-conditioned room with 12/12 h light/dark cycles for at least 1 week prior to the experiments. All of the swine had free access to a standard diet and water, and were fasted for 12 h but allowed water *ad libitum* before the experiment. The experimental protocols were approved by

National University of Singapore Institutional Animal Care & Use Committee.

fabrication of MN patch as described in the schematic shown in Fig. 1.

Coating of Glass Slide

Glass slides were coated in same way as described previously from our group (22, 23). Briefly, plain Corning micro slides (pre-cleaned, 75 × 50 mm, thickness: 0.96–1.06 mm) were coated with TMSPMA by soaking the slides for overnight, thereafter oven baked to get the coated slides. Coated glass slides were used further for

Fabrication of MN Patch

The fabrication was done in a similar way as described previously by our group, with slight modifications (22). It involves three steps as follows: 1) Fabrication of primary backing layer, 2) Fabrication of secondary backing layer and 3) Fabrication of the MN arrays. Schematic of the fabrication process has been shown in Fig. 1. The MN array, backing layer and MN were

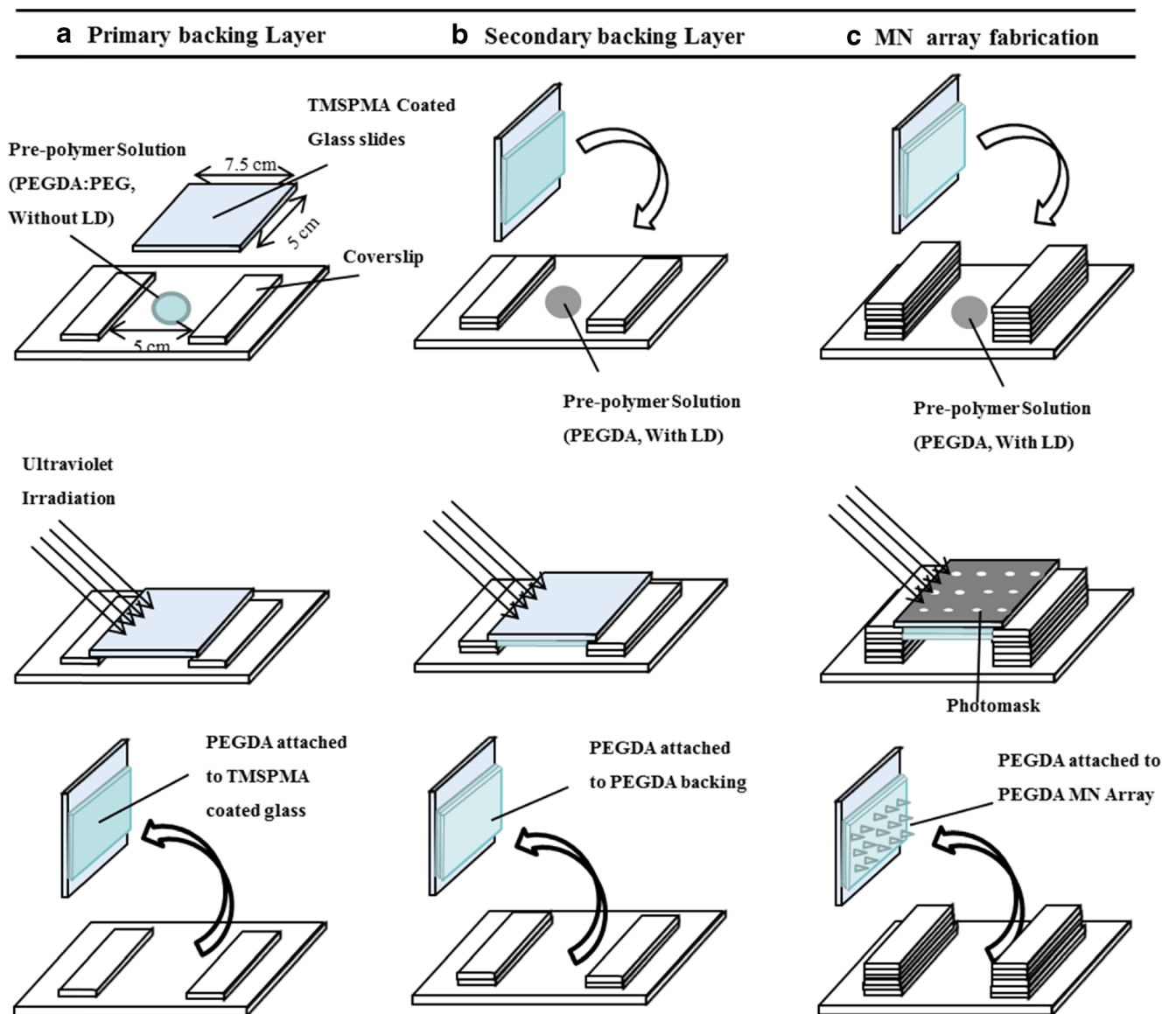


Fig. 1 Schematic representation of the fabrication process. (a) PEGDA is attached to TMSPMA coated coverslip via free radical polymerisation using ultraviolet (UV) irradiation, forming the primary backing. (b) PEGDA is attached to PEGDA primary backing to form secondary backing for MN array (c). PEGDA attached to PEGDA of secondary backing to form the Microneedle. All the set-up involves irradiation with UV light.

characterized using the stereoscopic microscope (Nikon SMZ25, Japan), using the measurement tools (like height) from Nikon imaging software (NIS-Element analysis D 4.20.00).

Primary Backing Layer

It was fabricated to facilitate the removal of final MN patch attached to coated glass slide. As shown in Table I, three ratios of PEGDA (with 0.5% *w/w* HMP): PEG 200 were evaluated to study the removal of MN patch using the blade, and to study oozing from the patch on keeping for 24 h at room temperature. Firstly, two coverslips (Mezel-Glasser 6 cm × 2.2 cm, #1.5) were stacked to the uncoated glass slide (each on either side) with 5 cm spacing between them. Then, the pre-polymer solution (PEGDA, containing 0.5% *w/w* HMP with PEG 200) was filled in the gap between two glass slides by wicking action. Later, the above setup was irradiated with UV light to photo polymerize the pre-polymer solution. Thereafter, glass slide with attached primary backing layer on its surface was removed from the setup. Subsequently, for the optimization of MN patch, UV irradiation parameters i.e. exposure time and variable distance of UV source at 100% intensity (10.9 W/cm²) were studied. The UV curing station (OmniCure S2000-XL, Canada) with a UV filter range of 320–500 nm, 8 mm liquid light guide and adjustable collimating adaptor was used for curing.

Secondary Backing Layer

It was fabricated in same manner as the fabrication of primary backing layer except for number of ‘spacer’ and composition of pre-polymer solution (PEDGA with 0.5% HMP and LD). The number of spacer was two for the secondary backing layer (two on each side) while it was one in the case of primary backing layer. The glass slide with primary backing layer was put on the setup as shown in Fig. 1. Then, the above setup was irradiated with the UV light.

Fabrication of MN Array

The set up for fabrication of MN array was similar to that used for backing layer fabrication except for the number of

‘spacers’ which was six in this case (six on each side). The composition of pre-polymer solution was same as that of secondary backing layer. Firstly, the glass slide with integrated primary and secondary backing layer was placed on the setup as shown in Fig. 1. Then, the above setup was irradiated with UV light. Thereafter, glass slide with fabricated MN patch was removed. Later, the MN patch was washed under running water for ~5 s to ensure removal of non-polymerized prepolymer solution, followed by cleaning using compressed air and then removed with the sharp blade to get 5 cm × 5 cm (25 cm²) size patch. As the washing was very quick and MNs were non-dissolving, this washing step would have cleared any amount of drug from the surface of the MN patch, but prevented any leakage of LD from the core of MNs. Four such patches were placed adjacent to each other and integrated as one using a scotch tape (Smith & Nephew, 10 cm × 4.5 m, stretched roll) to get 10 cm × 10 cm (100 cm²) size patch. MN patches using the prepolymer solution containing 2.2% (22 mg/ml), 15% (150 mg/ml) and 21% *w/v* (210 mg/ml) of LD were fabricated (21). All three concentrations of the LD in pre-polymer liquid formed clear solution.

Differential Scanning Calorimetry

Thermal analysis was done using the DSC (Universal V4.5A TA Instruments). 5 mg of sample was taken in the aluminum pan and pre-sealed before analysis using the clipper. The operating conditions for DSC were: heating rate 5°C / min; nitrogen gas flow rate 30 ml/min; and upper analysis temperature 120°C. The DSC thermograms were obtained and analyzed by using TA instrument software.

Mechanical Strength Testing

It was performed using an electronic force gauge (JSV H1000, JISC, Japan). The penetration efficiency and fracture force was determined using the force gauge as discussed before by Jaspreet *et al.* (21). To determine the fracture force, small array of MN (~1.5 cm²; after cutting from 25 cm² MN patch) was placed on the flat aluminum block which was placed against the moving force gauge, and to determine penetration efficiency; small MN array was placed on the full thickness skin,

Table I Effect of Backing Layer (BL) Composition to Facilitate Removal of Patch from the Glass Slide

Backing Layer (BL)	PEGDA (ml, with 0.5% <i>w/w</i> HMP)	PEG 200 (ml)	Facilitate Removal	Oozing
BL-1	9.0	1.0	×	×
BL-2	8.5	1.5	✓	×
BL-3	8.0	2.0	✓	✓

Where, ‘X’ shows did not facilitate the removal or did not lead to oozing, while ‘✓’, shows facilitate the removal or lead to oozing

then the force was applied with the force gauge. Force of the 10 N, 20 N, 30 N, 50 N and 70 N was applied to determine the penetration efficiency. In addition, numbers of MN intact or broken was also observed and percentage of the intact or broken MN was calculated.

In Vitro Skin Permeation

The skin permeation was carried out using the human cadaver skin for the various patches, i.e., MN-P1 (LD only in MNs), MN-P2 (LD in backing and MNs) and simple patch (without MNs). The skin was dermatome skin, donated by a 55-year-old, white male (Science Care, Phoenix, AZ, USA) with approval for use from National University of Singapore Institutional Review Board. All of that part of MN patch where LD was incorporated was fabricated using the prepolymer solution containing 21% of LD. The skin was first hydrated in PBS for 30 min, then measured using the scale and divided into equal portions using a sharp surgical blade. For each patch three replica of skin was taken for the permeation study. For the application of MN patches on the skin, 10 layers of Kim wipes was used as support, then the MN patch was applied with the force of a thumb on the side of the *stratum corneum* for 1 min. The MN array was then secured onto the skin using scotch tape, which was then mounted on vertical Franz diffusion cells with an effective exposed area of 1 cm². Then, the receptor cells were filled with 4.5 mL of PBS. Later, all diffusion cells were placed on the magnetic stirrer at 250 rpm in closed chamber maintained at 32°C by circulating hot air. At different time interval (for up to 24 h) full receptor liquid was replaced while collecting the samples into 2 ml Eppendorf tube. After completion of study, the skin tissue were digested and analyzed for the LD content. All samples were stored at 4°C after collection till the analysis was done. All the samples were centrifuged at 14,000 × *g* for 10 min at 4°C and the supernatant was used for analysis using validated HPLC method.

In Vivo Animal Study

Young adult female swine (Yorkshire X, Holland), ranging from 25 to 40 kg were used for the study. The animals were first sedated with ketamine (10 mg/kg), and then anesthetized with isoflurane gas followed by administration of Atropine to reduce salivary, tracheo-bronchial and pharyngeal secretions. While the animal was under anesthesia, hair and dirt on the swine skin at the intended application sites was removed prior to application of the patch. Subsequently, the hair was first clipped using an electric shaver followed by a wet disposable razor and patted dry. Later, the patch was applied using the hand without any use of applicator. After pasting the patch with the help of scotch tape, it

was pressed (normal hand force) with the palm for about 15 s. As the skin is not very flat, the applied vertical forces might not have been uniform. However, the base of MN patch was slightly flexible as compared to steel/aluminum block; it was also able to form a curved surface to adjust with the skin surface. Thereafter, animals were utilized for the preliminary plasma pharmacokinetics, *in vivo* permeation, lateral diffusion and skin irritation study as mentioned below. All animal testing procedures were done in accord with prior approval from the Institutional Animal Care and Use Committee, National University of Singapore.

Preliminary Animal Study

Firstly, a young adult female swine was anaesthetized as mentioned previously in “*In Vivo Animal Study*”. Before caring out the *in vivo* permeation test, lateral diffusion of drug was studied in addition to plasma pharmacokinetic to assess the possible interference in drug assay in relation to sites of applications of two patches if placed adjacent to each other. The large size ‘MN patch’ (100 cm²) was applied on the animal skin and fixed with scotch tape. Subsequently, at pre-determined time (10 min, 30 min, 1 h, 2 h, 4 h, 6 h, 8 h), blood samples were collected and stored at 4°C. At the end of 8 h, in addition to blood sample; skin biopsies were also collected similar to schematic as shown in Fig. 2.

The skin biopsies from site of patch application, and with certain distance from the boundary of the site of patch application were taken (2.5 cm, 5 cm and 10 cm). Later, the animal was euthanized with a high dose of Sodium Pentobarbital. After euthanasia, two full thickness biopsies of ~2 cm² were taken, one at the site where MN patch was applied and another one from the untreated skin. Both of the skin biopsies were stored separately in the 10% neutral buffer formalin (Sigma-Aldrich, USA) at 4°C and later utilized for histology study. All other biopsy samples were stored at -20°C until the analysis was done. Later, samples were processed and analyzed using the validated LC-MS/MS analytical method.

Histological Examination

The skin biopsies of MN treated and untreated skins were separately cross sectioned using the Microcryostat (Leica, Germany) to obtain cross sections of 30 μm. The cross sections were stained as per standard protocols of hematoxylin and eosin staining (H & E stain). The obtained stained samples were imaged and analyzed using the stereoscopic microscope (Nikon SMZ25, Japan) and the measurement tools of Nikon imaging software (NIS-Element analysis D 4.20.00).

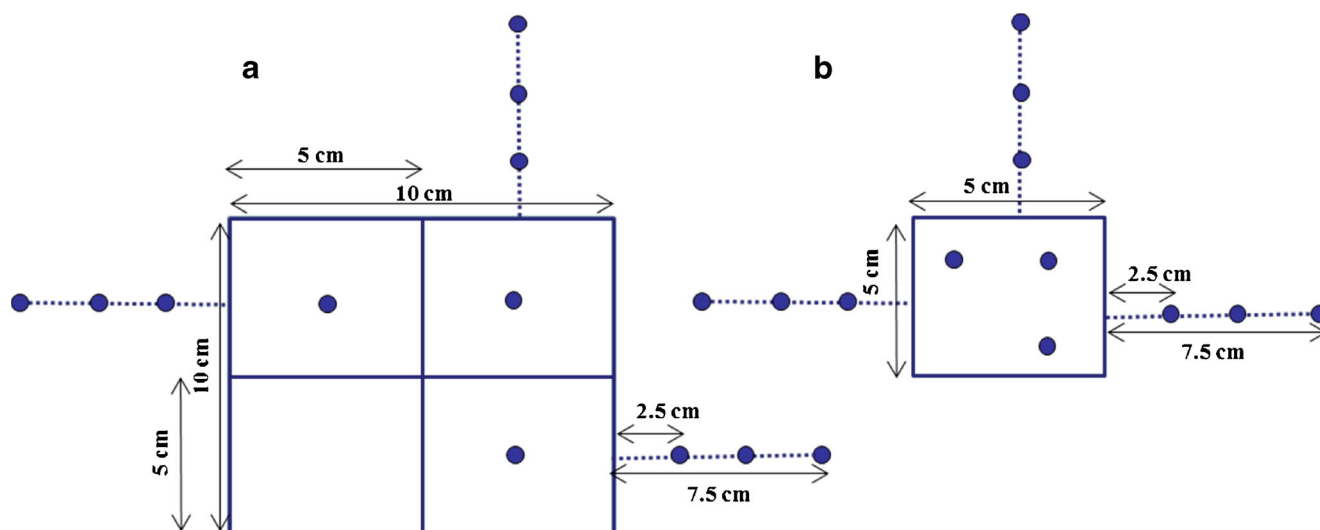


Fig. 2 Schematic of biopsies in and around the patch (a) 100 cm² MN-patch and control patch (b) 25 cm² MN-patch.

Plasma Pharmacokinetics

The objective of the plasma pharmacokinetics was to observe the amount of drug content which might be getting into the blood and may produce unwanted side effects like nausea, dizziness, drowsiness, etc. as it occurs commonly with use of the injections. Young adult female pigs were anaesthetized as mentioned previously in “*In Vivo Animal Study*”. Firstly, animals were divided into two groups, i.e., MN group and control group, each containing three animals. A commercial LD transdermal patch (containing 5% (50 mg/g) of LD) was used as control. The MN patch and control patch of 100 cm² was applied on the back area of each animal of their respective group, and fixed with scotch tape. At pre-determined time (10 min, 30 min, 1 h, 2 h, 4 h, 6 h and 8 h), 4.5 ml of blood samples were collected in 6 ml tubes (Vacuette; Austria) containing spray dried tri-potassium ethylene diamine tetra acetic acid (K3EDTA) as anticoagulant. Samples were collected via the catheter which was surgically inserted into the axillary vein. All samples were stored at -20°C until the analysis was done. Later, samples were processed and analyzed using the validated LC-MS/MS analytical method. Animals were rested for a week with normal feeding in controlled environment before being utilized for the further study.

In Vivo Skin Permeation and Lateral Diffusion

Young adult female pigs were anaesthetized as mentioned previously in “*In Vivo Animal Study*”. Each pig was utilized as single time point. Two MN patches of 100 cm² were applied on the back and loin region of the swine while two MN patches of 5 cm² were applied on the ramp and ham region of the swine. A commercial LD transdermal patch was used as control. On the opposite side of swine, two control patch of 100 cm² was applied on the back and loin region. All the

patches were kept at least 20 cm apart. At the end of predetermined time points (10 min, 30 min, 1 h, 2 h, 4 h, 6 h and 8 h), patch was removed. Immediately after the patch removal, skin was cleaned (thrice) with a cotton swab using PBS. Thereafter, a set of full thickness skin biopsies using sterile biopsy punches (Miltex USA, 4 mm) was collected in 2 ml Eppendorf tube from the site of patch application and sites with certain distance from the edge of patch as shown in Fig. 2. Separate biopsy punch was used for each biopsy. All samples were stored at -20°C until the analysis was done. Subsequently, the skin biopsies samples were subjected to processing and analyzed using the validated LC-MS/MS analytical method. Later, animals were euthanized with high dose of Sodium Pentobarbital. Precise time management was done to put the patches for collection of the biopsies at the end as biopsies collection for each time point for single patch takes about 5 min.

Skin Irritation

After each time points of the *in vivo* skin permeation and up to 8 h after the permeation study, skin was observed for any occurrence of erythema or edema. Each swine was having a small blank MN patch as control. General skin condition of swine was also observed on the subsequent 4 days after the patch removal. Signs of skin irritation, if any, was observed in accordance with skin reaction scores in laboratory animals (24).

Determination of Lidocaine Content

Sample Preparation

Blood samples: All the blood samples were harvested for plasma by centrifugation at $1000 \times g$ at 4°C for 10 min. One part

of plasma was treated with three parts of Methanol (containing prilocaine as internal standard (IS)) followed by mixing for 5 min using vortex mixer and then centrifuged at $14,000 \times g$ for 20 min at 4°C . Supernatant obtained was analyzed for drug content using validated LC-MS/MS method.

Skin Biopsies: Skin samples from the *in vitro* and *in vivo* studies were first digested using Proteinase K (75 $\mu\text{g}/\text{ml}$, 150 μl) to make homogenous mixture. Further details about working Proteinase K solution has been given in Table S1 (Supplementary Information). It was carried out at 55°C for 6 h. The obtained homogenous mixture was processed using protein precipitation method which was done by addition of three parts of methanol (containing prilocaine as IS), followed by mixing for 5 min using vortex mixer and then centrifugation at $14,000 \times g$ for 20 min at 4°C . The obtained supernatant was analyzed for drug content using validated LC-MS/MS method.

HPLC Method

The samples obtained from *in vitro* skin permeation were analyzed using HPLC (Hitachi L2000 LaChrome Elite) with quaternary pump and autosampler. 50 μl of sample (for each analysis) was injected into the Zorbax extended-C18 (4.6×75 mm, 3.5 μm) column protected with a guard column maintained at room temperature. The mobile phase composition was 35% of 25 mM ammonium hydroxide and 65% mixture (1:1) of iso-propyl alcohol with methanol in isocratic mode. The eluent was monitored by UV detector at 231 nm wavelength at flow rate of 1 ml/min. The calibration curve was plotted from 0.5 to 10 $\mu\text{g}/\text{ml}$ by running the LD standard solutions prepared in methanol.

LC-MS/MS Method

Quantitative analysis was done using Agilent 1200 series LC-MS/MS system, comprised of capillary pump, autosampler, and triple quadrupole mass detector (Agilent 6400 series). The data were acquired and processed using Mass hunter workstation software version B.02.01. The samples were analyzed using electrospray ionization (ESI) in positive ion mode with Turbo Ion Spray interface. The operating conditions were optimized using Mass Hunter optimizer for LD and IS-prilocaine, which were: dry gas temperature 350°C ; nebulizer pressure 35 psi; nitrogen gas flow rate 12 ml/min; capillary voltage 4000 V and fragmentor voltage 90 V. The product ions (of LD) resulting from transition of $235.2 \rightarrow 86.1$ (collision energy 16 V) and the product ions (of prilocaine) $221.2 \rightarrow 86$ (collision energy 8 V) were monitored at retention time of 3.1 min (for LD) and 2.4 min (for IS). 10 μl of sample (for each analysis) was injected into the Zorbax extended-C18 (4.6×75 mm, 3.5 μm) column protected with a guard column maintained at room temperature. The mobile

phase composition was 50% of 25 mM ammonium hydroxide and 50% mixture (1:1) of iso-propyl alcohol with methanol in isocratic mode at a flow rate of 0.5 ml/min. The calibration curve was plotted over the concentration range of 1–10,000 ng/ml (for plasma) and 10–1000 ng/ml (for skin) by running the standard solutions prepared in methanol from LD standard.

Statistical Analysis

The data were analyzed by using Microsoft Office Excel 2010 (Microsoft, Redmond, USA). All the results were presented as the mean \pm standard deviation. One-way analysis of variance (ANOVA) was performed to compare groups of data and *p*-values of less than 0.05 were considered statistically significant.

RESULTS

Effect of UV Irradiation

Both the exposure time and variable distance of UV source were found to affect the backing layers and MN properties. The optimized distance of UV source was 14 cm for all irradiations which includes primary backing layer, secondary backing layer and MN array. The optimized time of UV exposure was 4 s for both primary backing and secondary backing layer. The optimized time of UV exposure for MN array was 4.3 s and additional 2 s after washing and cleaning. It was found that if the UV source distance was kept below 14 cm, it was hardly possible to form the backing layers or MN array of $5 \text{ cm} \times 5 \text{ cm}$ (25 cm^2) size as it affect the area of UV exposure. If time of the UV exposure was less, for the backing layer it was found to cause incomplete polymerization leading to a gel-like layer. In the case of MN, UV exposure below the optimized level can result in soft gel-like needles with insufficient strength. In addition, the amount of PEG 200 (Table I) in the pre-polymer solution was found to affect the properties of backing layer (Figure S1, Supplementary Information).

Geometrical Properties of MN Patch

As shown previously by our group, MN properties are primarily controlled by the photomask dimensions (25, 26). The MN patch of 25 cm^2 with approximately 44 MN / cm^2 was fabricated. The thickness of integrated backing layer was $605 \pm 31 \mu\text{m}$, primary backing layer was $250 \pm 23 \mu\text{m}$ and secondary backing was $370 \pm 29 \mu\text{m}$. The length of MN $806 \pm 8 \mu\text{m}$, base diameter $316 \pm 4 \mu\text{m}$, tip diameter $265 \pm 7 \mu\text{m}$ and center-to-center spacing of $1455 \pm 14 \mu\text{m}$ was similar to the previously reported dimensions by our group (21). The images of the fabricated MN patch have been shown in Fig. 3.

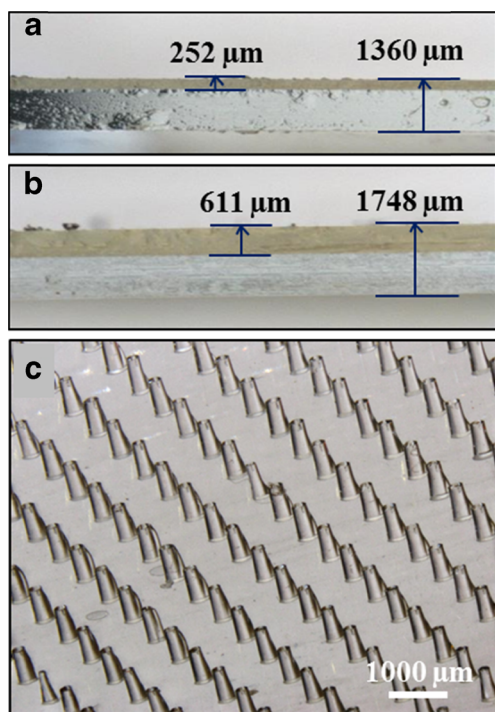


Fig. 3 Images of backing layers (on glass) and MN array of MN patch. (a) Primary backing layer (b) Secondary backing layer (c) MN array.

Mechanical Strength Testing

Fracture force of the MN patch was found to be 28 ± 3 N. It was comparatively less than that previously reported for the small size MN patch from our group (21). The percentage penetration efficiency for all types of MN patch was more than 90% at 10–30 N force and higher at the higher forces. The percentage of MN broken or intact is shown in Fig. 4.

At the force of 10–30 N, MN of more than 95% were intact on the patch for 21% LD containing patch, which was chosen for testing in pigs. The breakage of MN was observed to be 10–20% at force above 30 N. However, when the skin was observed after test, the broken MN or its parts were found to be on the skin surface or on the superficial layer of the skin and was easily wiped off with tissue papers.

Differential Scanning Calorimetry

The calorimetry was performed to study the physical state of LD within the MN patch. The blank MN and MN containing 21% LD showed similar thermogram as shown in Fig. 5. The absence of endothermic drug peaks showed that drug inside the MN matrix was amorphous; however, LD itself is crystalline in nature. The amorphous nature revealed that LD was completely dispersed & solubilized in the MN matrix. Therefore, it should also be uniformly distributed. Furthermore, the observation that the prepolymer solution (containing 21% w/v of LD) formed clear solution in addition

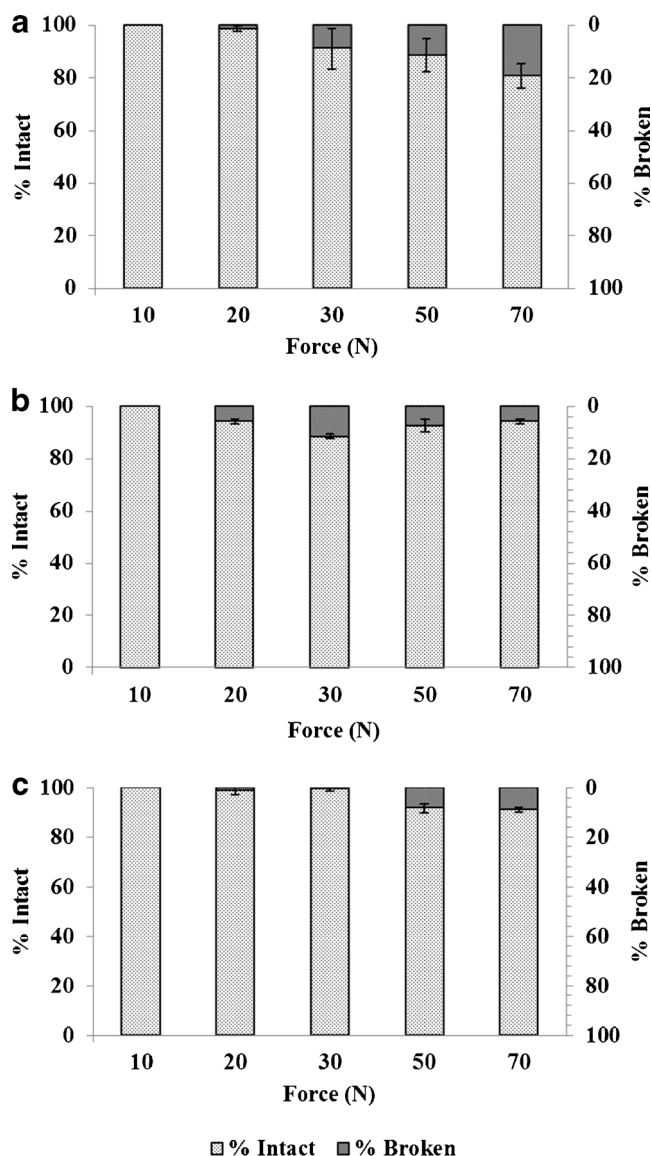


Fig. 4 MN Strength of MN patches in form of percentage of MN intact and broken during penetration testing on full thickness skin, when lidocaine was encapsulated at (a) 2.2% (w/w), (b) 1.5% (w/w) and (c) 21% (w/w).

to DSC thermogram ensures the uniform distribution of the LD in the MN patch matrix.

In Vitro Skin Permeation

Figure 6b shows the *in vitro* skin permeation of various patches (MN-P1, MN-P2 and simple patch). The permeation was found to be fastest and highest in the MN-P2 as compared to other two patches. It shows a biphasic skin permeation profile, with the first phase being burst permeation for about 1 h and the second phase being a sustained permeation for about 24 h. While MN-P1 also showed biphasic permeation, the extent of permeation in both phases was much less than that of the MN-P2 due to the amount of LD content which

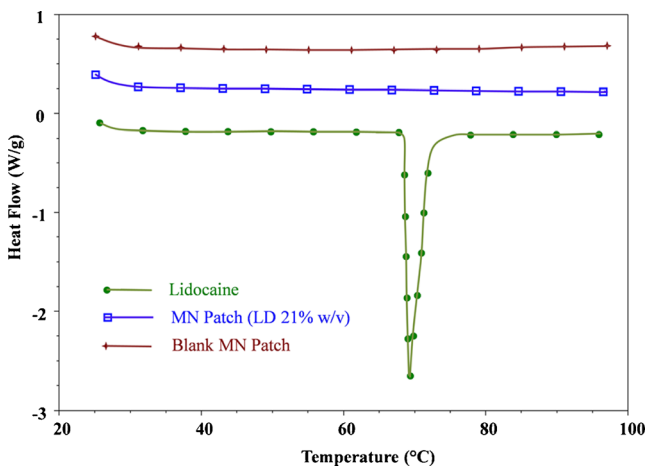


Fig. 5 DSC thermograms of Lidocaine, blank MN patch, MN patch with 21% w/v LD.

was less as compared to MN-P2. The ‘simple patch’ showed an initial lag phase of ~20–30 min during which there was no permeation of LD. Both of the MN patches (MN-P1 and MN-P2) showed faster permeation than the simple patch during the initial phase. Figure 6c shows the cumulative LD trapped in the skin and permeated through the skin after 24 h time period. It showed that MN-P2 has the highest overall permeation than the simple patch of same material and same LD content. Both MN-P1 and simple patch showed almost same amount of the LD trapped in skin after 24 h. However, the overall skin permeation was less in case of the MN-P1 because of the absence of LD in backing layer.

Histological Examination

Histological section with H & E staining is shown in Fig. 7, specifically with the depth of penetration of MN in Fig. 7b and c. The depth of penetration of the MNs were in the range of 210–380 μm (Figure S2, Supplementary Information) for various histological section studied (in general, <400 μm). The depth of penetration was variable for various histological sections from the same skin biopsy because of non-uniform vertical forces applied as a cause of non-flat skin surface and large size patch.

Plasma Pharmacokinetic

Plasma collected from the blood samples showed the presence of drug peaks at some time points for both control as well as MN-patch. However, the concentrations were below the lowest limit of quantification (1 ng/ml) of the LC-MS method. The low amount of LD in systemic circulation indicated that the use of MN patch can circumvent the potential systemic side effects associated with the use of LD injections. It also showed that topical applied LD was mainly distributed inside skin.

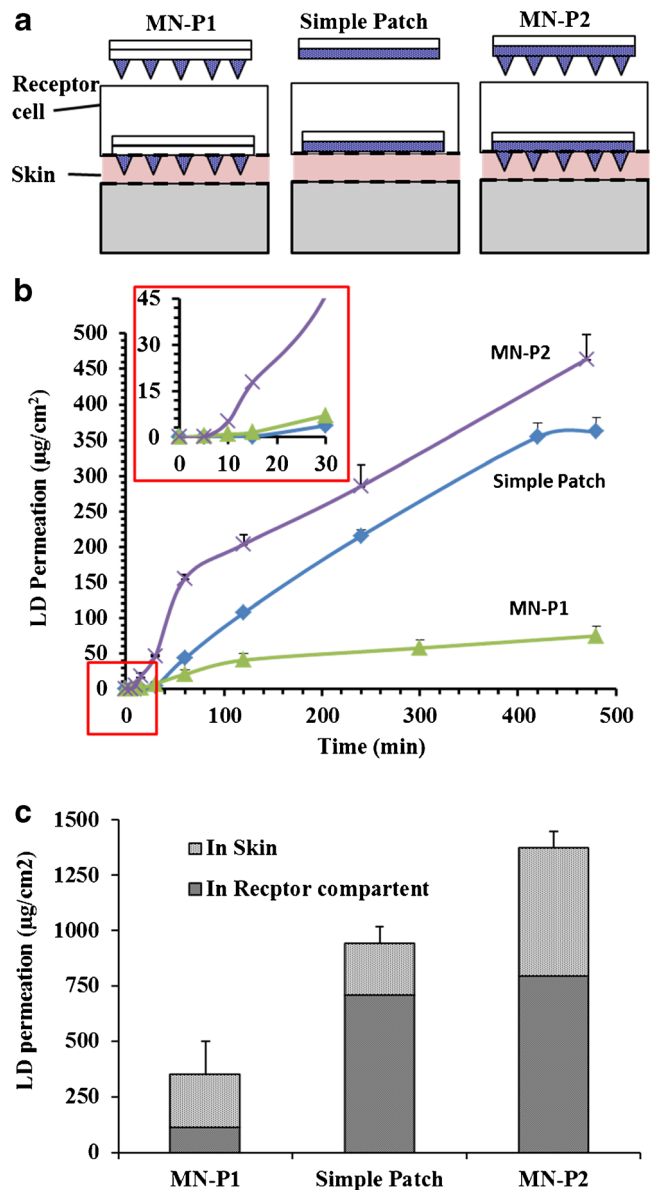


Fig. 6 *In vitro* skin permeation of various patches (MN-P1, simple patch and MN-P2). (a) Schematic of patches (blue colored region shows the presence of LD). (b) *In vitro* skin permeation (c) Cumulative lidocaine content permeated and inside the skin after 24 h.

In Vivo Skin Permeation

It has been reported that a commercial patch (5% w/w LD) gave an onset of pain relief after 30 min of application (27). Therefore, the amount of LD permeated into the skin in 30 min for the commercial patch was considered to be an approximation for the LD therapeutic level. It was estimated to be ~53 $\mu\text{g}/\text{cm}^2$. Zhang, Y. *et al.* has also determined the therapeutic level of LD using similar method using EMLA cream (5% LD) which has been reported to start its action at around 1 h after application (20). The *in vivo* skin permeation as shown in Fig. 8 revealed that both 25 cm^2 and 100 cm^2 MN patches could achieve the therapeutic level at the first

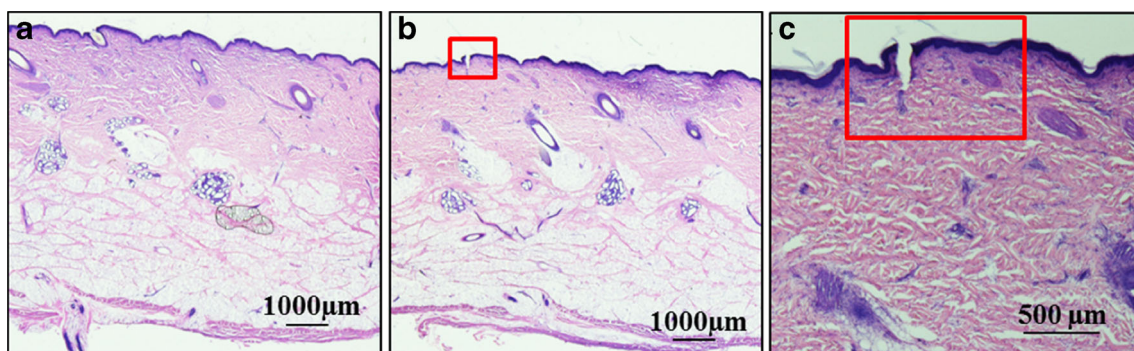


Fig. 7 Histological section of pig skin after H & E staining. **(a)** Intact pig skin (without MN patch application). **(b)** Punctured skin (after MN patch application for 8 h). **(c)** Magnified image of punctured skin.

sampling point i.e. 10 min. The extent of LD permeation was found higher for 100 cm² MN at all-time points as compared to 25 cm² patch. However, both patches showed similar skin permeation profiles. But compared with control, the 100 cm² MN-patch showed 11 fold higher and 25 cm² MN-patch showed 9 folds higher skin permeation at 10 min. The large size 100 cm² MN patches maintained the therapeutic level throughout the 8 h of study. For the 25 cm² MN patches, they maintained therapeutic level throughout the 8 h of study, except for the 30 min sampling point.

Lateral Diffusion

The lateral diffusion was found to be highest for the 100 cm² MN-patch followed by 25 cm² MN-patch and finally, the control patch. The trend was obvious and could be directly correlated to the trend of LD skin permeation under the patch as shown in Fig. 9 and Table II. The higher skin permeation for 100 cm² showed the higher lateral diffusion as well. The LD content was found to decrease with distance from the site of the patch application.

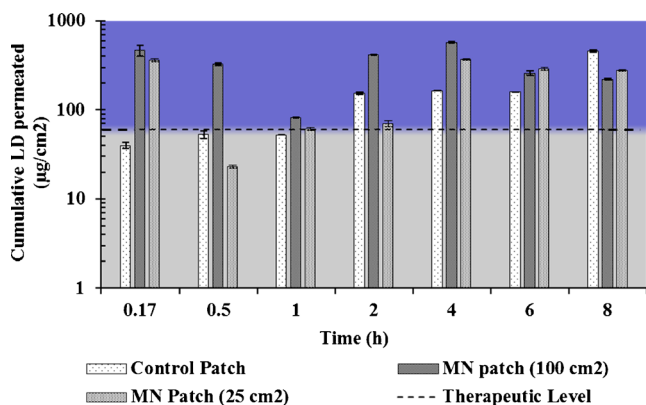


Fig. 8 *In vivo* skin permeation in control patch, 25 cm² MN-patch and 100 cm² MN-patch. Dark blue region shows above therapeutic level region while light blue shows below therapeutic level region.

Skin Irritation Test

The signs of needle penetration can be seen in the MN patch as compared to normal shaved skin and the control patch (Fig. 10). There was no visible sign of inflammation, erythema or edema for up to 6 h of application. In a few pigs slight redness was observed at 8 h but disappeared within 24 h after patch removal (Fig. 10).

DISCUSSION

The fabrication of large MN patch using photolithography approach can be a suitable alternative to other methods of fabrication like micro molding where fabrication requires high temperature and/or heat (28). If the large MN patch was fabricated with only one backing layer, it would be very hard to remove the MN-patch from its substrate, i.e., the coated glass slide. To help in the removal process of the large size MN patch, PEG 200 was incorporated in the primary backing layer (29). The easy removal of MN patch with embedded PEG 200 may be attributed to the absence of the ability to form covalent links with TMS-PMA coating on the glass slide. In addition, plasticizing effect of the PEG 200 may have made the backing layer relatively flexible which aids in the easy removal of MN patch. However, this property of PEG 200 also gave rise to the need of a secondary backing layer because it caused a reduction in the strength of MN array.

The length of MNs was ~800 µm. As a fact, for maintaining the concentration of LD in the skin to allow sustained pharmacological action, the depth of penetration should not be as high as 800 µm due to the presence of capillary network in the papillary dermal region (at ~1 mm depth) (30, 31). It should be just sufficient to create micropunctures but avoids the blood capillaries; hence, preventing sudden clearance of the drug. However, the depth of penetration and length of microneedle are not necessarily the same as it varies with tip diameter, force of application, length of MN, etc. (32).

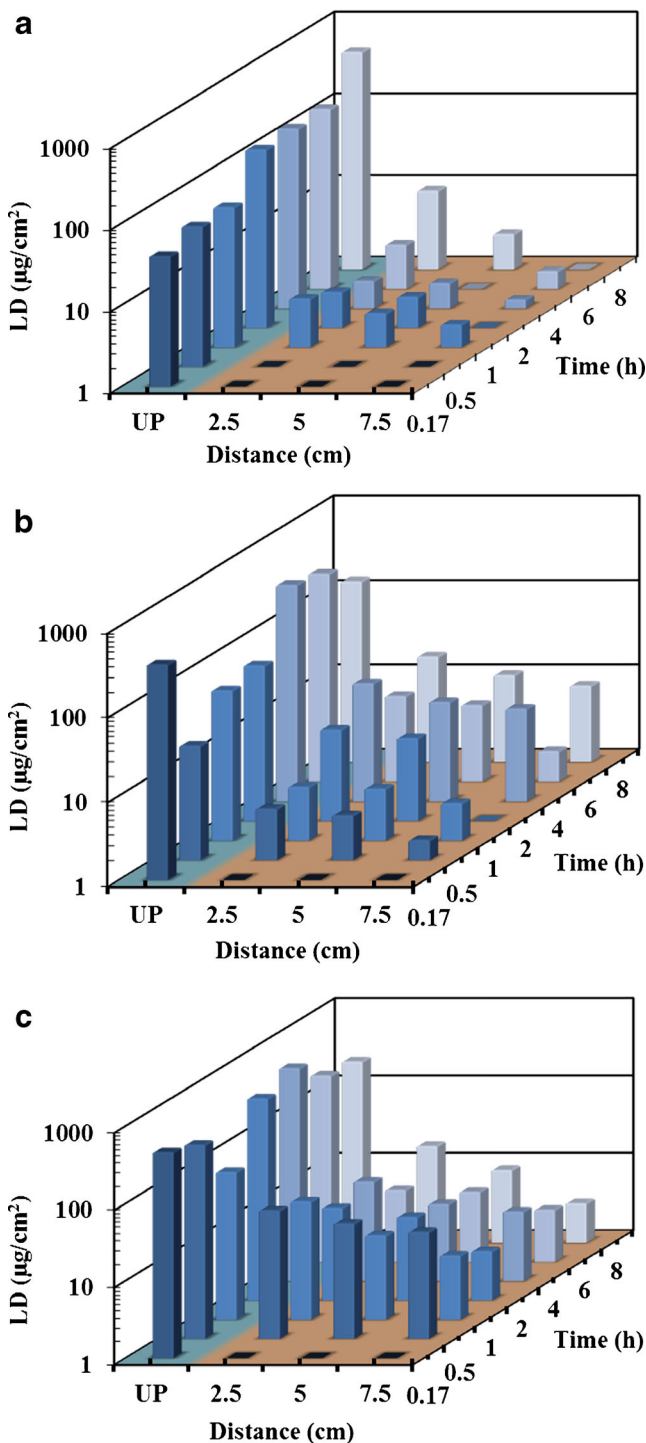


Fig. 9 Time dependent lateral diffusion in various patches (a) control patch, (b) 25 cm² MN-patch and (c) 100 cm² MN-patch. Where, blue colored region shows LD permeation under patch (UP) and brown region shows the lateral diffusion of LD from the region beyond patch application.

Moreover, the depth of penetration of microneedle ranges widely from 10 to 80% of the microneedle length (25,

32–35). The penetration of the needles was less than 400 µm as shown in Fig. 7. In addition, the plasma pharmacokinetic study did show the presence of only very low amount of LD at some time points. Therefore, it can also avoid the side effects which may occur with the use of LD injections.

The DSC thermogram shown in Fig. 5 revealed that the physical state of LD inside the MN patch was completely amorphous even at high concentration, i.e., 21% w/v. The complete solubilization and a DSC thermogram support uniformity of the drug inside the matrix of the MN-patch. This ensures the consistent and sustained release of LD from the MN-patch for the consistent therapeutic actions.

In the *in vitro* skin permeation study, the biphasic skin permeation pattern for MN-P1 and MN-P2 was observed as in Fig. 6. The initial fast release (up to 1 h) could be attributed to fast permeation through the micro perforations created by the MN array loaded with LD. In the later phase, sustained linear permeation could be attributed to passive and lateral bilayer diffusion which was known to be the primary pathway of permeation for the drugs through intact skin (36) and less extent through the perforated skin. The fast permeation in the initial phase (majority from LD loaded in the MN) through the perforated skin can also be supported by the absence of the initial phase in the ‘simple patch’ as skin perforations were not generated. The higher extent of LD permeation in case of ‘simple patch’ than the MN-P1 can be attributed to low drug loading in MN-P1. This further support the fall of *in vivo* permeation observed as shown in Figs. 8 and 9, at time point 30 min in case of the small patch and 1 h in case of 100 cm² patch.

The 11 fold and 9 fold higher permeation of LD for MN-patches at 10 min was evident of the fast onset of MN patches. The fall in concentration observed in permeation as shown in Figs. 8 and 9, at time points 30 min in case of the small patch and 1 h in the case of 100 cm² patch may be attributed to the biphasic release from the patch resulting in biphasic skin permeation. It showed fast permeation at the initial phase of permeation, followed by fall in permeation i.e. middle phase and then sustained permeation i.e. the second phase of permeation. The fast permeation can be attributed to the absorption of drug via micro-pores created after application of the MN patch while the later sustained release would have been an outcome of persistent absorption. D’Alvise *et al.* has shown metabolism of LD converting to 3-OH-lidocaine in subcutaneous tissue and white adipose tissue surrounding the hair follicles, which might also lead to a fall in *in vivo* permeation other than the lag between biphasic release of the MN patch (37).

The absence of quantifiable drug peak in plasma showed the tendency of the LD to be localized and distributed within the skin layers to produce local analgesia. Moreover, it implied the rare chances of systemic toxicity, which may occur with use of intravenous injections.

Table II LD Permeation/Lateral Diffusion ($\mu\text{g}/\text{cm}^2$) at Different time Intervals for Control Patch, 25 cm^2 MN Patch and 100 cm^2 MN Patch. UP Represent the LD Skin Permeation, While; 2.5, 5 and 7.5 Represent the Lateral Diffusion of LD at Distance of 2.5 cm, 5 cm and 7.5 cm, Respectively

LD permeation ($\mu\text{g}/\text{cm}^2$) at different time (h) intervals							
Location	0.17	0.5	1	2	4	6	8
Control Patch							
UP	39.81 \pm 24.64	52.6 \pm 37.11	52.36 \pm 2.31	152.98 \pm 38.48	159.66 \pm 1.43	159.66 \pm 2.44	456.88 \pm 127.01
2.5	NA	0.59 \pm 0.01	3.99 \pm 1.18	2.77 \pm 1.85	2.18 \pm 0.11	3.45 \pm 4.88	9.2 \pm 1.98
5	NA	0.59 \pm 0.12	2.62 \pm 0.71	2.42 \pm 1.38	2.05 \pm 1.03	0.89 \pm 1.26	2.69 \pm 1.12
7.5	NA	0.44 \pm 0.09	1.91 \pm 0.87	0.94 \pm 0.79	1.29 \pm 0.15	1.65 \pm 2.34	0.69 \pm 0.58
25 cm^2 microneedle patch							
UP	355.22 \pm 91.46	22.82 \pm 7.94	60.13 \pm 15.73	69.08 \pm 48.41	364.33 \pm 48.45	286.47 \pm 81.80	136.55 \pm 193.11
2.5	NA	4.09 \pm 0.51	4.35 \pm 4.82	12.06 \pm 4.61	24.79 \pm 7.65	10.25 \pm 9.69	17.51 \pm 3.30
5	NA	3.42 \pm 0.58	4.14 \pm 4.34	9.54 \pm 0.41	14.93 \pm 5.31	8 \pm 7.81	10.59 \pm 4.80
7.5	NA	1.74 \pm 0.61	2.79 \pm 1.89	NA	12.43 \pm 7.75	2.29 \pm 1.53	7.95 \pm 3.92
100 cm^2 microneedle patch							
UP	459.88 \pm 498.09	322.36 \pm 88.44	80.79 \pm 2.67	408.97 \pm 42.66	565.86 \pm 110.81	255.48 \pm 110.86	218.49 \pm 36.45
2.5	NA	45.94 \pm 50.58	33.89 \pm 16.84	15.75 \pm 3.14	19.24 \pm 15.74	8.44 \pm 1.60	17.67 \pm 2.13
5	NA	31.1 \pm 31.55	12.34 \pm 4.81	11.99 \pm 0.81	9.93 \pm 6.31	8.02 \pm 1.16	8.61 \pm 1.89
7.5	NA	24.3 \pm 25.51	6.73 \pm 2.37	4.33 \pm 3.89	7.93 \pm 5.09	4.72 \pm 2.32	3.23 \pm 1.23

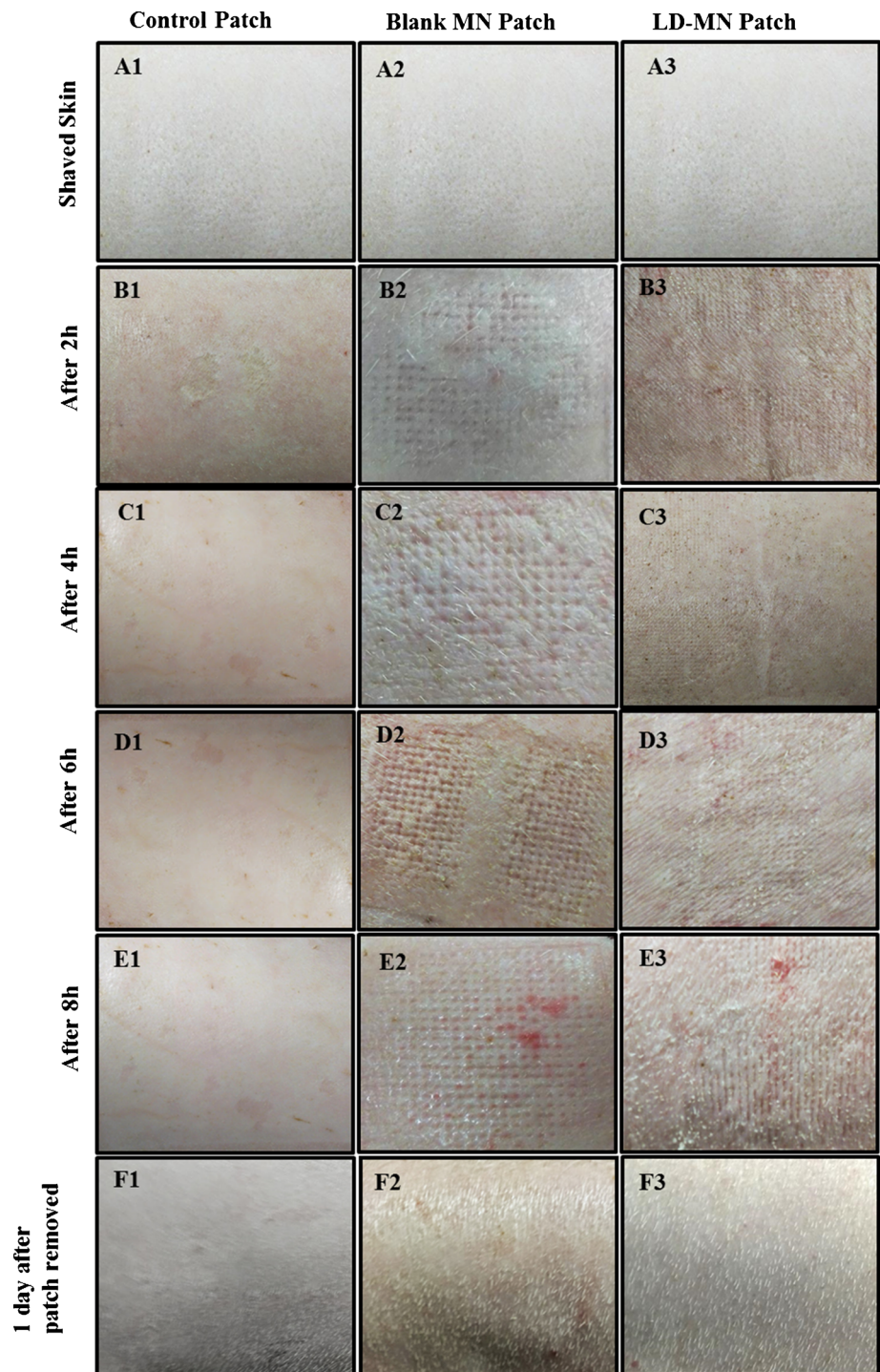
It revealed that patch size and type can alter the extent of permeation and lateral diffusion. As observed in Figs. 8 and 9, the MN-patch of two different sizes showed different extent of the skin permeation and lateral diffusion. In general for all types and size of patches, initial time point i.e., 10 min, the LD was either not quantifiable or not detected in the sample obtained from outer sites of applied patch site. Later, small MN patch showed lower recovery of the LD from outer sites of applied patch site as compared to larger MN patch which showed higher recovery. The higher recovery in large MN patch can be attributed to higher permeation than the small patch. However, the control patch shows least lateral diffusion among the three patches though being equivalent in size to the larger patch. This could be attributed to the slow skin permeation of LD through control patch because of slow absorption by passive diffusion, absence of micro needling feature, and another reason could be because of low loading of LD (5%).

LD was recovered up to 7.5 cm from the lateral parts outside of applied patch site. However, the previous report showed the lateral diffusion for about less than 2 cm as most of results were either *in vitro* or only studied the *stratum corneum* (38–40). Therefore, the lateral diffusion observed *in vivo* after analyzing full thickness skin biopsies showed different observations from the previous report. Bellas *et al.*, has also emphasized on use of the full thickness 3D skin for topical studies (41). Though follicular transport (37) of LD has also been reported, the study by Johnson, M. E. *et al.* (36) and lateral diffusion for such a long distance supports the bilayer lateral diffusion as the primary mechanism for the LD absorption. This also

suggests the localization of LD was primarily in the skin as plasma pharmacokinetic study showed either absence or non-quantifiable LD in the blood stream. The continuous spatial distribution of LD including both lateral and forward transport supports the continuous supply of the LD from the patches to maintain the therapeutic level beside its other possible reduction pathways like metabolism (37) and drug clearance (42).

The *in vitro* biocompatibility of polymeric MN array alone has been shown previously by our group using three different cell lines which include human dermal fibroblasts (HDF), human adult low calcium high temperature (HaCaT) cells, and human embryonic kidney 293 (HEK293) cells (43). However, significant differences were observed between the cellular model and porcine model. As shown in Fig. 10, no visible signs of irritation were observed up to 6 h of application. However, minor sign of skin reaction has been observed after 8 h of application. PEG 200 which was absent in the previous but present in current MN experiment has been reported in literature to be safe for topical use (44). The reason for skin irritation had not yet been recognized. However, the skin seems to recover within 24 h as signs of irritation disappeared. The absence of skin irritation in the initial 6 h and minor irritation at 8 h may be an attribute for the time dependent diffusion of toxic substance. In such case, the dissolving MN might have a greater safety concern than the non-dissolving MN as the mechanism of permeation would

Fig. 10 Skin irritation test images of control patch (A1-F1), blank MN patch (A2-F2) and LD-MN patch (A3-F3).



have been dissolution (faster) rather than diffusion (slower). Therefore, in the case of non-dissolving MNs, such possible toxicity may be avoided by reducing the time of application. Furthermore, the use of topical antioxidant either simultaneously or after the application of patch can also ameliorate toxicity as shown by Abhimanyu Sabnis *et al.* (45).

CONCLUSION

The large size polymeric MN patch containing LD has been fabricated by photolithography. It shows majority of LD diffuses perpendicularly against skin, with little lateral diffusion. Most of the permeated drug resides within the site of application. The patch is potentially useful for fast and sustained

delivery of LD to alleviate both acute and chronic pain. Particularly, it can be useful to geriatric and pediatric population for pain management as an alternative to injections with effectiveness and convenience.

ACKNOWLEDGMENTS AND DISCLOSURES

The authors thank the National University of Singapore veterinary staff for their support for the animal studies. This study was supported by the Singapore National Research Foundation grant NRF-POC-R-148-000-178-281.

REFERENCES

- Golzari SE, Soleimanpour H, Mahmoodpoor A, Safari S, Ala A. Lidocaine and pain management in the emergency department: a review article. *Reg Anesth Pain Med.* 2014;4(1), e15444.
- Tauzin-Fin P, Bernard O, Sesay M, Biais M, Richebe P, Quinart A, *et al.* Benefits of intravenous lidocaine on post-operative pain and acute rehabilitation after laparoscopic nephrectomy. *J Anaesthesiol Clin Pharmacol.* 2014;30(3):366–72.
- Fujii H, Fukushima T, Ishii M, Nagano Y, Kawanishi S, Watanabe Y, *et al.* The efficacy of intravenous lidocaine for acute herpetic pain—placebo controlled trial. *Masui.* 2009;58(11):1413–7.
- Hellgren U, Kihamia CM, Premji Z, Danielson K. Local anaesthetic cream for the alleviation of pain during venepuncture in Tanzanian schoolchildren. *Br J Clin Pharmacol.* 1989;28(2):205–6.
- Bai Y, Miller T, Tan M, Law LS, Gan TJ. Lidocaine patch for acute pain management: a meta-analysis of prospective controlled trials. *Curr Med Res Opin.* 2015;31(3):575–81.
- Wilson JR, Kehl LJ, Beiraghi S. Enhanced topical anesthesia of 4% lidocaine with microneedle pretreatment and iontophoresis. *Northwest Dent.* 2008;87(3):40–1.
- Nayak A, Babla H, Han T, Das DB. Lidocaine carboxymethylcellulose with gelatine co-polymer hydrogel delivery by combined microneedle and ultrasound. *Drug Deliv Rev.* 2016;23(2):658–69.
- Nayak A, Das DB, Vladislavjevic GT. Microneedle-assisted permeation of lidocaine carboxymethylcellulose with gelatine co-polymer hydrogel. *Pharm Res.* 2014;31(5):1170–84.
- Oni G, Brown SA, Kenkel JM. Can fractional lasers enhance transdermal absorption of topical lidocaine in an in vivo animal model? *Lasers Surg Med.* 2012;44(2):168–74.
- Sammeta SM, Repka MA, Narasimha MS. Magnetophoresis in combination with chemical enhancers for transdermal drug delivery. *Drug Dev Ind Pharm.* 2011;37(9):1076–82.
- Rao R, Nanda S. Sonophoresis: recent advancements and future trends. *J Pharm Pharmacol.* 2009;61(6):689–705.
- Singer AJ, Homan CS, Church AL, McClain SA. Low-frequency sonophoresis: pathologic and thermal effects in dogs. *Acad Emerg Med.* 1998;5(1):35–40.
- Tu X, Yin Q, Zhang W, Huang H. The progress of research on low-frequency sonophoresis and its applications. *Sheng Wu Yi Xue Gong Cheng Xue Za Zhi.* 2008;25(6):1474–8.
- Ernst AA, Pomerantz J, Nick TG, Limbaugh J, Landry M. Lidocaine via iontophoresis in laceration repair: a preliminary safety study. *Am J Emerg Med.* 1995;13(1):17–20.
- Gagliano-Juca T, Castelli MR, Mendes GD, Arruda AM, Chen LS, de Oliveira MA, *et al.* Pharmacokinetic and pharmacodynamic evaluation of a nanotechnological topical formulation of lidocaine/prilocaine (nanorap) in healthy volunteers. *Ther Drug Monit.* 2015;37(3):362–8.
- Cazares-Delgadillo J, Naik A, Kalia YN, Quintanar-Guerrero D, Ganem-Quintanar A. Skin permeation enhancement by sucrose esters: a pH-dependent phenomenon. *Int J Pharm.* 2005;297(1–2):204–12.
- Hu L, Silva SM, Damaj BB, Martin R, Michniak-Kohn BB. Transdermal and transbuccal drug delivery systems: enhancement using iontophoretic and chemical approaches. *Int J Pharm.* 2011;421(1):53–62.
- Lee PJ, Langer R, Shastri VP. Role of n-methyl pyrrolidone in the enhancement of aqueous phase transdermal transport. *J Pharm Sci.* 2005;94(4):912–7.
- Stahl J, Kietzmann M. The effects of chemical and physical penetration enhancers on the percutaneous permeation of lidocaine through equine skin. *BMC Vet Res.* 2014;10:138.
- Zhang Y, Brown K, Siebenaler K, Determan A, Dohmeier D, Hansen K. Development of lidocaine-coated microneedle product for rapid, safe, and prolonged local analgesic action. *Pharm Res.* 2012;29(1):170–7.
- Kochhar JS, Lim WX, Zou S, Foo WY, Pan J, Kang L. Microneedle integrated transdermal patch for fast onset and sustained delivery of lidocaine. *Mol Pharm.* 2013;10(11):4272–80.
- Kochhar JS, Goh WJ, Chan SY, Kang L. A simple method of microneedle array fabrication for transdermal drug delivery. *Drug Dev Ind Pharm.* 2013;39(2):299–309.
- Kathuria H, Fong MH, Kang L. Fabrication of photomasks consisting microlenses for the production of polymeric microneedle array. *Drug Del Trans Res.* 2015;5(4):438–50.
- Tardiff RG, Hubner RP, Graves CG. Harmonization of thresholds for primary skin irritation from results of human repeated insult patch tests and laboratory animal skin irritation tests. *J Appl Toxicol.* 2003;23(4):279–81.
- Kochhar JS, Quek TC, Soon WJ, Choi J, Zou S, Kang L. Effect of microneedle geometry and supporting substrate on microneedle array penetration into skin. *J Pharm Sci.* 2013;102(11):4100–8.
- Kathuria H, Kochhar JS, Fong MH, Hashimoto M, Iliescu C, Yu H, *et al.* Polymeric microneedle array fabrication by photolithography. *J Vis Exp.* 2015;105, e52914. doi:10.3791/52914.
- Rowbotham MC, Davies PS, Verkempinck C, Galer BS. Lidocaine patch: double-blind controlled study of a new treatment method for post-herpetic neuralgia. *Pain.* 1996;65(1):39–44.
- Kim YC, Park JH, Prausnitz MR. Microneedles for drug and vaccine delivery. *Adv Drug Del Rev.* 2012;64(14):1547–68.
- Sothornvit R, Krochta JM. Plasticizer effect on oxygen permeability of beta-lactoglobulin films. *J Agric Food Chem.* 2000;48(12):6298–302.
- Gupta J, Felner EI, Prausnitz MR. Minimally invasive insulin delivery in subjects with type 1 diabetes using hollow microneedles. *Diabetes Technol Ther.* 2009;11(6):329–37.
- Tuan-Mahmood TM, McCrudden MT, Torrisi BM, McAlister E, Garland MJ, Singh TR, *et al.* Microneedles for intradermal and transdermal drug delivery. *Eur J Pharm Sci.* 2013;50(5):623–37.
- Romgens AM, Bader DL, Bouwstra JA, Baaijens FP, Oomens CW. Monitoring the penetration process of single microneedles with varying tip diameters. *J Mech Behav Biomed Mater.* 2014;40:397–405.
- Coulman SA, Birchall JC, Alex A, Pearton M, Hofer B, O'Mahony C, *et al.* In vivo, in situ imaging of microneedle insertion into the skin of human volunteers using optical coherence tomography. *Pharm Res.* 2011;28(1):66–81.
- Crichton ML, Ansaldo A, Chen X, Prow TW, Fernando GJ, Kendall MA. The effect of strain rate on the precision of penetration of short densely-packed microprojection array patches coated with vaccine. *Biomaterials.* 2010;31(16):4562–72.
- Kochhar JS, Anbalagan P, Shelar SB, Neo JK, Iliescu C, Kang L. Direct microneedle array fabrication off a photomask to deliver collagen through skin. *Pharm Res.* 2014;31(7):1724–34.
- Johnson ME, Blankschtein D, Langer R. Evaluation of solute permeation through the stratum corneum: lateral bilayer diffusion as the primary transport mechanism. *J Pharm Sci.* 1997;86(10):1162–72.

37. D'Alvise J, Mortensen R, Hansen SH, Janfelt C. Detection of follicular transport of lidocaine and metabolism in adipose tissue in pig ear skin by DESI mass spectrometry imaging. *Anal Bioanal Chem.* 2014;406(15):3735–42.
38. Gee CM, Nicolazzo JA, Watkinson AC, Finnin BC. Assessment of the lateral diffusion and penetration of topically applied drugs in humans using a novel concentric tape stripping design. *Pharm Res.* 2012;29(8):2035–46.
39. Schicksnus G, Muller-Goymann CC. Lateral diffusion of ibuprofen in human skin during permeation studies. *Skin Pharmacol Physiol.* 2004;17(2):84–90.
40. Nayak A, Short L, Das DB. Lidocaine permeation from a lidocaine NaCMC/gel microgel formulation in microneedle-pierced skin: vertical (depth averaged) and horizontal permeation profiles. *Drug Del Trans Res.* 2015;5(4):372–86.
41. Bellas E, Seiberg M, Garlick J, Kaplan DL. In vitro 3D full-thickness skin-equivalent tissue model using silk and collagen biomaterials. *Macromol Biosci.* 2012;12(12):1627–36.
42. Cevc G, Vierl U. Spatial distribution of cutaneous microvasculature and local drug clearance after drug application on the skin. *J Control Res.* 2007;118(1):18–26.
43. Kochhar JS, Zou S, Chan SY, Kang L. Protein encapsulation in polymeric microneedles by photolithography. *Int J Nanomedicine.* 2012;7:3143–54.
44. Polyethylene glycol [MAK Value Documentation, 1998]. In: *The MAK-Collection for Occupational Health and Safety*: Wiley-VCH Verlag GmbH & Co. KGaA; 2002. p. 248–270.
45. Sabnis A, Rahimi M, Chapman C, Nguyen KT. Cytocompatibility studies of an in situ photopolymerized thermoresponsive hydrogel nanoparticle system using human aortic smooth muscle cells. *J Biomed Mater Res A.* 2009;91(1):52–9.